CREEP FRACTURE PARAMETERS OF FUNCTIONALLY GRADED COATING

Jian-Jun Chen and Shan-Tung Tu*

ABSTRACT

Functionally graded coating (FGC) has been widely used in severe conditions for its excellent mechanical characteristics compared with pure coating material. The graded component in the FGC can be described by specified local volume fraction rules of coating material. In this paper an inhomogeneous finite element method is used to investigate the crack behavior in FGC at elevated temperature with the power-law constitutive equation. The path- independent integral value C^* characterizes amplitude of the crack tip stress fields at steady stage. Different volume fractions of coating material, creep coefficients and creep indices are analyzed by systematic computation to obtain the effects of these factors on crack growth and obtain the knowledge to minimize crack damage in the FGC. In addition, strain energy density rate factor, Λ, is proposed as a material parameter for measuring crack resistance capability in creep conditions. The preliminary analysis with Λ is also applied in FGC and the numerical results showed that Λ can also characterize the coating load capacity.

Key Words: functionally graded material, creep crack, C^*, strain energy density rate factor.

I. INTRODUCTION

By painting with heat barrier or corrosion-proof coating, the substrate material can be protected in an aggressive environment, reliably and safely. However, the different mechanical properties between coating and substrate will introduce significant residual or thermal stresses in the interface of bonds, reduce the coating/substrate fracture strength, and decrease the predicted design life severely (Tu, 2002). The concept of functionally graded coating was put forward by Niino (Niino and Maeca, 1990) first in 1990 to tackle the mismatch in the coating/substrate system. The coating generally consists of several intermediate layers with spatial variances in properties. If the microstructure and components in the coating are varied smoothly, from one material to another material in thickness direction, this advanced coating is thus called functionally graded coating (FGC). Functionally graded coating can be produced according to performance requirements to minimize hazardious mis-match stress to within the allowed levels. Due to the broad prospective usage of FGC its fabrication method has been investigated and corresponding research work about mechanical behavior has been done in both theory and experiment, extensively. Pioneering analysis in nonhomogeneous material mechanics has been done by Atkinson (Atkinson and List, 1978) and elastic fracture problems of functionally graded materials are solved by Erdogan (1995). Based on those works Noda (Noda and Jin, 1993) considered the additional thermal load in FGMs. Although functionally graded coating, currently, is used mostly in high temperature applications, literature referring to the creep behavior of FGC are limited. Williamson (Williamson *et al*., 1995) analyzed the creep effects of graded ceramic-metal only concerning the strain distribution, taking no account of the fracture mechanics. Biner (1998) has investigated interface cracks in a creep regime with simplified interlayer model, but his model

*Corresponding author. (Tel: +86 21 64253425; Email: stu@ecust.edu.cn)

J. J. Chen is with the School of Mechanical Engineering, East China University of Science and Technology, Shanghai 200237, China.

S. T. Tu is with the School of Mechanical and Power Engineering, Nanjing University of Technology, Nanjing 210009, China.

is not a strict graded material model. In view of the importance of the creep behavior of FGC the present study is focused on creep behavior of cracks in coatings. The coating is graded in terms of the continual variation of the volume fraction from one material (i.e. ceramic) at the surface to another material – substrate material (i.e. metal) at the bond interface. The substrate is assumed to be a homogeneous, isotropic material and the bond region is regarded as an ideal interface. The local volume fraction obeying the power law type is investigated and the mechanical parameters of the coat are obtained using the rule of mixtures. Moreover, the strain energy density rate factor is introduced and applied to solve the FGC problems.

II. ANALYSIS OF THE FUNCTIONALLY GRADED COATING

1. Constitutive Model

At high temperature the strain rate of the material undergoing creep deformation is generally analyzed by using the Norton power law:

$$\dot{\varepsilon}=B\sigma^n \tag{1}$$

where $\dot{\varepsilon}$ and σ are the von Mises equivalent strain rate and stress respectively, B and n are the material constants. The amplitude of stress-strain fields near the crack tip is associated with the contour integral $C(t)$ (Moran and Shih, 1987). By analogy with the form of the J-integral, the $C(t)$ is defined as:

$$C(t)=\int_{\Gamma\to 0}[\dot{W}dy-T_i(\frac{\partial \dot{u}_i}{\partial x})ds] \tag{2}$$

where T_i is the component of the traction vector; u_i the displacement rate vector component; $\dot{W}$ is strain energy rate density and is given by

$$\dot{W}=\int_0^{\dot{\varepsilon}}\sigma d\dot{\varepsilon} \tag{3}$$

The integral path Γ should be sufficiently small to assure the elastic strain rates are negligible compared with creep strain rates around the crack tip.

Once the material is extensively under creep conditions, that means steady state creep dominates the ligament region ahead of the crack tip, the long-time value of $C(t)$ is then designated as another path-independent integral value: C^*. The role of $C(t)$ or C^* can be referred to a characterizing parameter of creep crack initiation and subsequent quasi-static growth in viscoelastic solids (Bassani and McClintock, 1981).

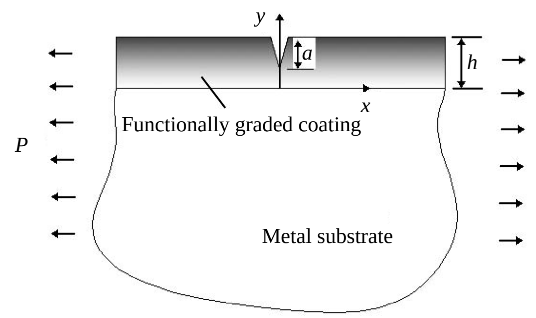

(a) Cartesian coordinate

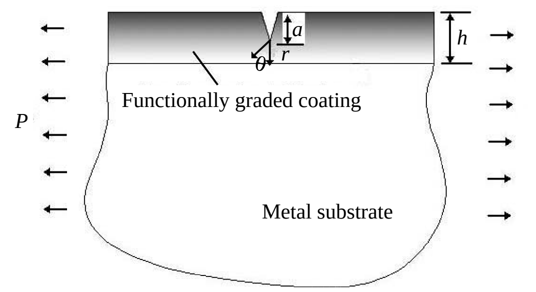

(b) Polar coordinate

Fig.1 Coating and substrate system

2. Coating Parameters

The local volume fraction determines the graded material property and can be controlled by regulating the ratios of two materials in mixture. Understanding the effects of volume fractions is the foundation to FGC analysis. A local coordination illustrated in Fig.1a is used in the present paper to characterize the space variation of the volume fraction. For convenience the x-axis lies within the interface and the y-axis is set along the coating thickness direction. In the present study volume fractions of the coating material $f(y)$ are assumed to obey the power law function. Because in the interface (y=0) the coating material does not exist while in the coating surface (y=h) the component is pure coating material, the power law function thus can be simplified as follows:

$$f(y)=(y/h)^{\alpha} \tag{4}$$

the total volume fraction of coating material is then given by

$$g=\frac{1}{h}\int_0^h f(y)dy=\frac{1}{h}\int_0^h (y/h)^{\alpha}dy=\frac{1}{\alpha+1} \tag{5}$$

In (Bao and Wang, 1995) Bao pointed out that the effective properties of a functionally graded material can be obtained using the rule of mixtures as a first order approximation. So the effective Young's module $E(y)$, Poission's Ratio $\nu(y)$, creep coefficient

$B(y)$, creep index $n(y)$ in FGC can be expressed as

$$E(y)=f(y)E_c+[1-f(y)]E_s=E_s+f(y)[E_c-E_s] \tag{6}$$

$$\nu(y)=f(y)\nu_c+[1-f(y)]\nu_s=\nu_s+f(y)[\nu_c-\nu_s] \tag{7}$$

$$B(y)=f(y)B_c+[1-f(y)]B_s=B_s+f(y)[B_c-B_s] \tag{8}$$

$$n(y)=f(y)n_c+[1-f(y)]n_s=n_s+f(y)[n_c-n_s] \tag{9}$$

Konda and Erdogan (1994) pointed out that the effect of the Poisson's ratio in graded material is negligible. A value of 0.3 was used for Poisson's ratio in all cases in the present analysis.

3. Inhomogeneous Finite Element Method

Several numerical methods have been used to investigate FGC, including integral equations (Konda and Erdogan, 1994), the higher order model (Aboudi *et al*., 1999), boundary elements (Goldberg and Hopkins, 1995), and finite elements (Eischen, 1987; Drake *et al*., 1993). In this paper an inhomogeneous finite element method is employed to calculate the stress-strain fields of the graded coating. The finite element formulation is discussed below.

In an inhomogeneous finite element method the strain increment of the element $\Delta\boldsymbol{\varepsilon}^{(e)}$ can be determined by the displacement of the node $\Delta\boldsymbol{\delta}^{(e)}$ as:

$$\Delta\boldsymbol{\varepsilon}^{(e)}=\boldsymbol{B}^{(e)}\Delta\boldsymbol{\delta}^{(e)} \tag{10}$$

$\boldsymbol{B}^{(e)}$ is the element strain-displacement matrix. The relationship between incremental strain and stress in the two dimensional problem is

$$\Delta\boldsymbol{\sigma}^{(e)}=\boldsymbol{D}^{(e)}(x, y)\Delta\boldsymbol{\varepsilon}^{(e)} \tag{11}$$

where $\boldsymbol{D}^{(e)}(x, y)$ is the constitutive matrix, which is the function of position for material. According to the principle of virtual work, the basic equation of a finite element method boundary value problem can be described as follows

$$\boldsymbol{k}^{(e)}\Delta\boldsymbol{\delta}^{(e)}=\Delta\boldsymbol{P}^{(e)}+\Delta\boldsymbol{Q}^{(e)} \tag{12}$$

where $\Delta\boldsymbol{P}^{(e)}$ is the incremental load vector (including thermal load) and $\Delta\boldsymbol{Q}^{(e)}$ represents the incremental pseudo-loads vector due to creep strain. The element stiffness matrix $\boldsymbol{k}^{(e)}$ and the pseudo-creep-loads vector $\Delta\boldsymbol{Q}^{(e)}$ are defined respectively as

$$\boldsymbol{k}^{(e)}=\int_{\Omega}[\boldsymbol{B}^{(e)}]^T\boldsymbol{D}^{(e)}(x, y)\boldsymbol{B}^{(e)}d\Omega \tag{13}$$

$$\Delta\boldsymbol{Q}^{(e)}=\int_{\Omega}[\boldsymbol{B}^{(e)}]^T\boldsymbol{D}^{(e)}(x, y)\Delta\boldsymbol{\varepsilon}_c^{(e)}d\Omega \tag{14}$$

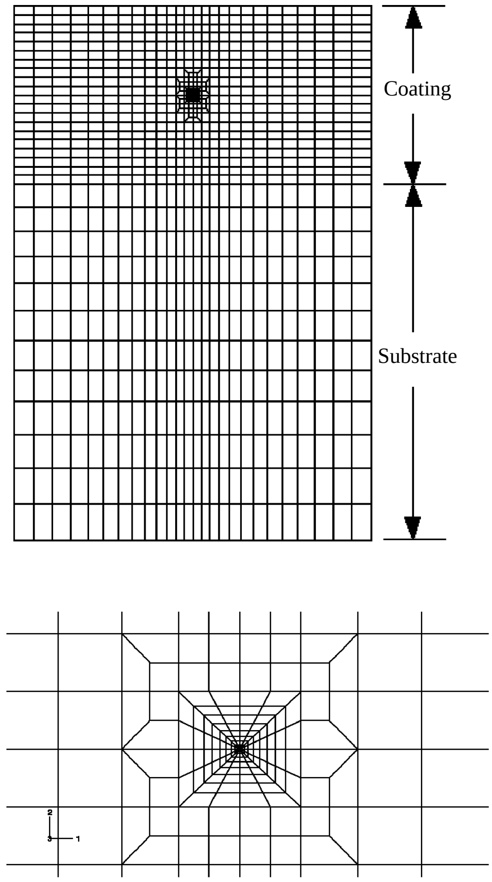

Fig. 2 Entire mesh and detail mesh at the crack tip

in which Ω is the element domain and $\Delta\boldsymbol{\varepsilon}^{(e)}$ is the increment of creep strain. The above reasoning, at the element level, can be readily extended to the whole domain of the structure. Because inhomogeneous elements can represent the continuous variation of the material parameters, it especially fits graded material (Zhang and Leech, 1985). Compared with general methods, such as homogeneous finite element analysis, the present method can acquire the same accurate results with fewer elements and use less computer time.

Finite element analysis is performed by using the commercial code ABAQUS and a user defined inhomogeneous eight nodes bi-quadratic reduced integration element is employed for the whole coating/substrate system except at the crack tip where a collapsed bi-quadratic reduced element is used. Through the programmed element the graded properties can be realized in the element inside. The mesh near the crack tip is refined to ensure the final C^* obtained from different contours will converge to the same value. The entire mesh and detailed mesh at the crack tip are illustrated in Fig. 2. The remote load with the amplitude 130KN is applied to the coat/substrate system

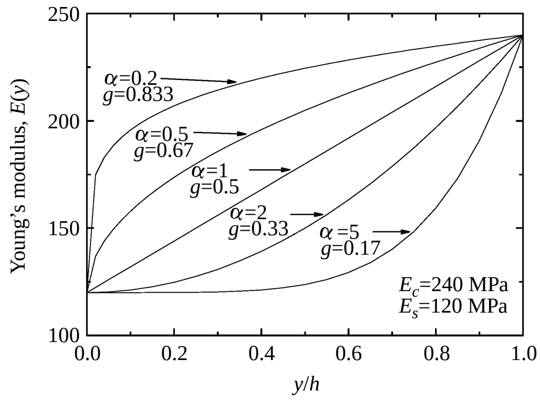

Fig. 3 Distribution of Young's module in the graded coating

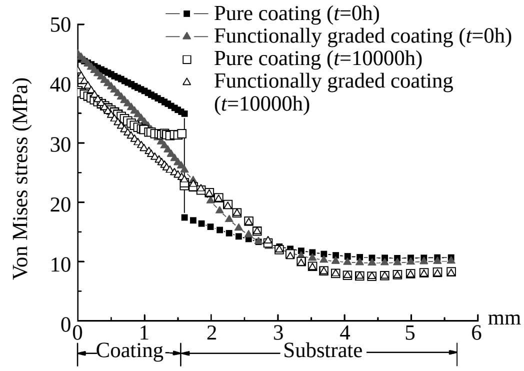

Fig. 4 Stress at interface

in the x-direction as illustrated in Fig. 1a. All the analyses presented in this study are carried out under this identical applied load level and the elastic properties of pure coating and substrate material are taken to be E_c/E_s=2.0 and ν_c/ν_s=1.0. The distribution of mechanical parameters in the functionally graded coating follows the rules discussed above (Fig. 3).

III. RESULT AND DISCUSSION

The stress field distribution of the pure coating/ substrate and graded coating/ substrate are simulated first without consideration of cracks. Due to the different mechanical parameters of the pure coating and substrate, the mismatch stress at the interface is significantly severe compared to the graded coating/ substrate.

From Fig. 4 it can be seen that in pure coating/ substrate case the stress near the interface is discontinuous. The amplitude of von Mises stress on the coating side is almost twice the stress on the substrate side of the interface. The existence of stress mismatch is the major factor to cause the cracking of coating systems in service. However this undesirable state does not occur in functionally graded coatings. No abrupt variation of stress indicates more load capacity and higher fracture strength in coating. Thus the benefit of using FGC is definitely offered here.

To reveal the influence of coating gradation on crack initiation and growth, systematic schemes are made to compute C^* in term of the different correlation factors and the C^* can be normalized as follows:

$$\frac{C^*}{\sigma_0 \varepsilon_0 h} = \gamma(\frac{B_s}{B_c}, \frac{h_s}{n_c}, \frac{a}{h}, \alpha) \qquad (15)$$

where σ_0 and ε_0 are the initial remote stress and strain level when the external load is applied and the influence of γ on E_s/E_c, ν_c and ν_s are left implicit.

Because C^* can be regarded as the fracture parameter which controls the amplitude of the stress field at the crack tip, then smaller γ means lower stress level in the graded coating and more load capacity remains.

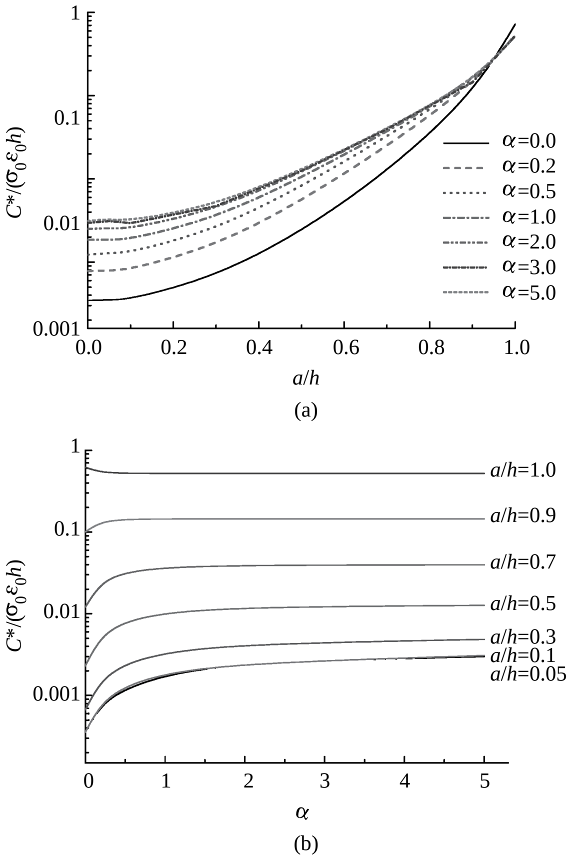

Fig. 5 Influence of local volume fraction

The influence of local volume fraction on C^* is illustrated in Fig. 5(a). The creep coefficient B of substrate and coating is 1.0e-15 and 1.0e-16 respectively and creep index is assumed to be 5.0 identically. With the increment of crack length a/h,

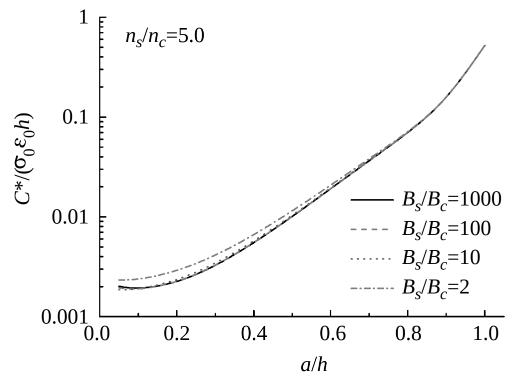

Fig. 6 Influence of creep coefficient B

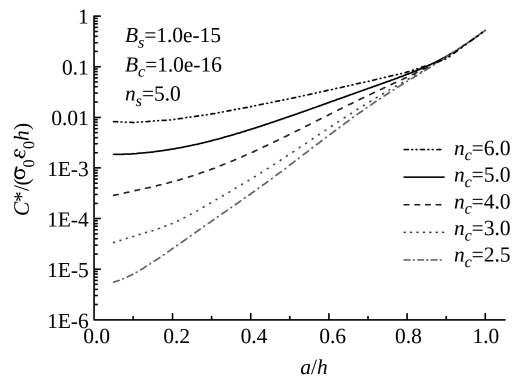

Fig. 7 Influence of creep index n on the C^*

normalized value $C^*/\sigma_0\varepsilon_0 h$ increases with diverse rates in terms of different volume fraction exponents α. The volume fraction exponent α in Eq. (4) represents the inhomogeneity of the coating material. The case α=0 indicates that the coating is made of a homogeneous material and has no graded components diversification. In the present study pure coating material has better fracture toughness than the substrate material so the curve α=0 is located lower than other curves along most other ranges of crack length. However when crack length a/h goes up to 1.0, that means the crack tip lies exactly at the bimaterial interface, the incompatible mechanic properties cause more stress concentration than the stress in graded material and make the curve α=0 larger than other curves. From Fig. 5(a) it can be seen besides the α=0 curve all other curves with different volume fraction exponents converge to the same value when a/h reaches unity. This means the increment of crack length in the material before the crack tip gradually becomes similar as the substrate material and the advanced graded coating material reduce synchronously. Along with the crack progress the different stress field distribution caused by varied α vanishes. It also can be seen that with the same crack length, the normalized value $C^*/\sigma_0\varepsilon_0 h$ increases concurrently with the increment of α. That indicates minor α is beneficial to prevent cracking occurrences in the coating surface and such character is especially advantageous for corrosion-proof coating, because the surface of corrosion-proof coating contacts the aggressive environment directly and cracks initiate in that location first. From Fig. 6(a) it also can be noticed that when α>3 the gaps between the curves are minimal and the change of volume fraction has no effect on the load capacity of the functionally graded coating.

To further explore the influence of the volume fraction on the crack driving force (C^*), the normalized value $C^*/\sigma_0\varepsilon_0 h$ is plotted as a function of volume fraction exponents α for different crack lengths in Fig. 5(b). It can be seen that the curve of crack length a/h=0.05 is almost coincident with the curve of crack length a/h=0.1 no matter how the α value changes. While the crack length a/h>0.1 the gaps between each curve are evident.

The relationship between creep coefficient ratio B_s/B_c and $C^*/\sigma_0\varepsilon_0 h$ at different crack lengths is shown in Fig. 6. It is worth noting that the value of the creep coefficient ratio has small influence on the coating's loading capacity. When $2\le B_s/B_c\le 10$ the dependence of $C^*/\sigma_0\varepsilon_0 h$ on the creep coefficient ratio value is very small and when B_s/B_c>10 the effect of creep coefficient ratio on fracture driving force is nearly zero. These results are important to the design of FGM coating for use at elevated temperature. For FGM with a certain crack the load capacity is not sensitive to the creep coefficient, which means in material choice there is no need to pay much attention to the creep coefficient of the coating. Therefore an optimal design of FGM coating can be obtained by mainly considering the other mechanical properties such as material creep index etc.

A plot of the normalized value $C^*/\sigma_0\varepsilon_0 h$ as a function of crack length a/h is shown in Fig. 7 for different creep indices. Different from the creep coefficient, the creep index has an important influence on the fracture driving force of the graded material.

With the crack progress, the $C^*/\sigma_0\varepsilon_0 h$ value increases monotonously under a given creep index. Finite element calculations show the crack driving force is higher when the coating material has a higher creep index. This result is more explicit in the shallow crack case and with the crack length (a/h) increasing, the curves with different creep indices converge gradually. When the crack tip is near the coating/substrate interface the crack driving forces caused by different creep indices are nearly identical. This means lower creep index of coating material can benefit the whole system load capacity in shallow cracks but can not enhance mechanical performance in deep cracks.

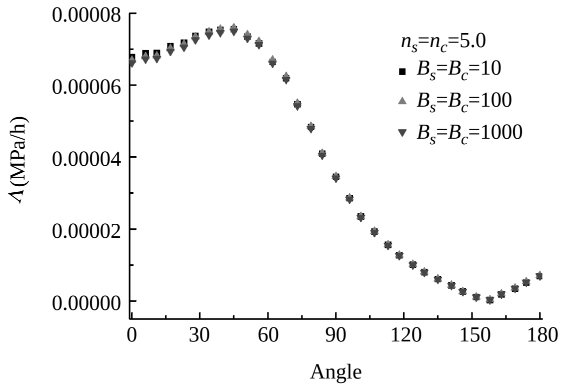

Fig. 8 Influence of creep coefficient B on strain energy density rate factor

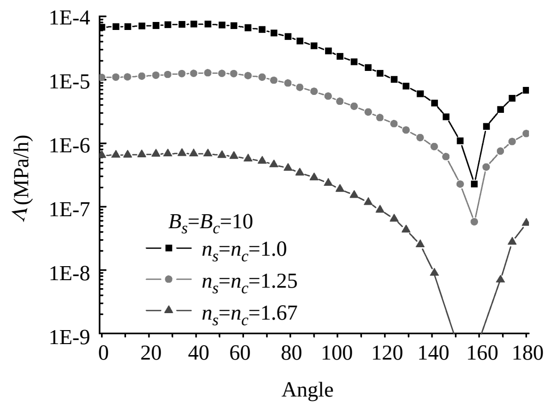

Fig. 9 Influence of creep index n on strain energy density rate factor

IV. STRAIN ENERGY DENSITY RATE FACTOR

The strain energy density factor theory established by Sih (1974) has been successfully used as a fracture criterion in several practical fields. In comparison with the global integral parameter, J, the strain energy density factor S is able to predict the crack growth direction and kinetic angle of propagation. It is defined as:

$$\frac{S}{r} = \frac{dW}{dA} = \int_{r \to r_0} \sigma_{ij} d\varepsilon_{ij} \tag{16}$$

where W is the strain energy density and r is the radial distance measured from the crack tip. The critical value r_0 is usually postulated to be 1/10 of the crack length. Although the S concept is initially used in LEFM, it can easily extended to resolve non-linear elastic fracture problems.

Under the extensive steady-state creep condition Goldman and Hutchinson (1975) derived the relationship between stress, strain rate and the C^* integral parameter. From their work the amplitude of stress and strain rates around the crack tip are only concerned with the coordinates of the site and can be determined by a formula containing the angular function defined by Rice and Rosengren (1968). This resembles the HRR fields at the crack tip of a power law hardening material and makes it possible to introduce a new local fracture parameter following the concept of strain energy density factor, which is designated as “strain energy density rate factor”, Λ.

In the analogy, strain in Eq. (16) is replaced by the strain rate and the product value $\sigma_{ij} d\dot{\varepsilon}_{ij}$ is calculated at the polar distance r_0. Then the strain energy density rate factor Λ can be expressed as follows:

$$\frac{\Lambda}{r} = \frac{d\dot{W}}{dA} = \int_{r \to r_0} \sigma_{ij} d\dot{\varepsilon}_{ij} \tag{17}$$

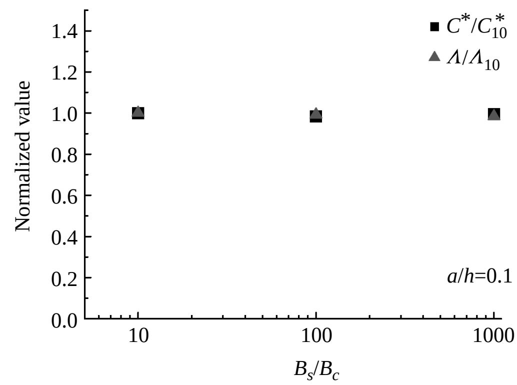

Fig. 10 Normalized value of C^* and Λ at different creep coefficient ratios

To verify the availability of parameter Λ in functionally graded coating, the above analyzed FGC/substrate model is reused except when Cartesian coordinates are replaced by polar coordinates (Fig. 1b). The influence of the creep coefficient ratio B_s/B_c on the strain energy density rate factor Λ is illustrated in Fig. 8. It can be seen that Λ varies as a function of the polar angle θ. The difference in the creep coefficient ratio has small effect on Λ value, which is the same as the result of C^* analyzed above.

Fig. 9 shows Λ versus polar angle θ with the crack length a/h=0.1 at different creep index ratios. Unlike the relationship between Λ and creep coefficient ratio, the dependence of creep index ratio on Λ is seen to be quite strong.

This consequence also agrees with the above numerical results analyzed by C^*.

To quantitatively explore the relationship between Λ and C^*, their normalized values are given in Fig. 10 and Fig. 11 to show the influence caused by different creep coefficient ratios and creep index ratios. In both figures the Λ is designated as the value at the location θ=0°, where Λ=max{$\Lambda|\partial\Lambda/\partial\theta$=0 and

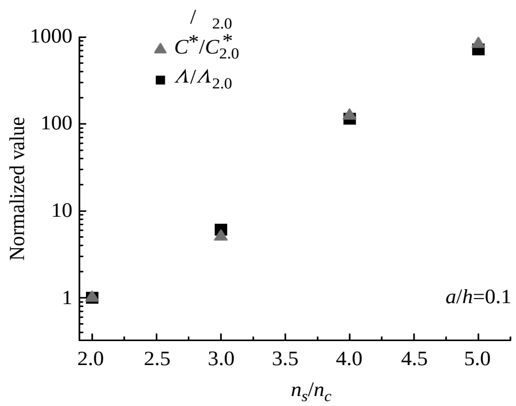

Fig. 11 Normalized value of C^* and Λ at different creep index ratios

$\partial^2\Lambda/\partial\theta^2>0\}$. In the two figures C^*_{10}, Λ_{10}, $C^*_{2.0}$ and $\Lambda_{2.0}$ represent the corresponding value of the case B_s/B_c=10 and n_s/n_c=2.0 respectively.

It can be seen that the two kinds of normalized values exactly fit each other. This means the various coating performances caused by different creep coefficient ratios or creep index ratios can be represented by the Λ value.

V. CONCLUSIONS

Functionally graded coatings have aroused great interest in researchers and engineers in the last decade for outstanding performance under severe conditions. The smooth distribution of graded components prevents the mismatch stress caused by different mechanical properties in the interface. Due to the gradual change of microstructure, the mechanical behavior of the FGC is extremely complex. Although some analytic results have been obtained in linear elastic frameworks, it is still impossible to give exact solutions for nonlinear elastic material. The present work focuses on the graded coating mechanical performance under creep conditions and tries to uncover the relationship between constitutive coefficients and coating behavior. A systematic finite element calculation has been carried out and several conclusions can be drawn as below:

1) Smaller volume fraction exponent is beneficial to prevent cracking in the coating surface; The α should generally be smaller than 2, in order to reduce the crack sensitivity on the surface of the FGC;
2) The creep coefficient ratio, B_s/B_c, has little effect on the crack driving force of the FGC;
3) The crack driving force is very sensitive to the creep exponent ratio, n_s/n_c. Lower creep exponent in the coating material is beneficial to the load capacity of the coating/substrate system
4) Strain energy density rate factor can be used to characterize the FGC system and should be a better choice for the future study of micro- or nano-coating system.

Although in the present paper, the material creep coefficient and index are designated to the given value, the results and above analysis method can be extended to other graded coating systems with similar distribution rules of mechanical properties.

ACKNOWLEDGMENTS

This work is supported by the China Natural Science Foundation (Contract Nos. 50225517 and 10172046) and the authors are grateful to Prof. G. C. Sih for his invaluable advice.

REFERENCES

Aboudi, J., Pindera, M. J., and Arnold, S. M., 1999, "Higher-Order Theory for Functionally Graded Materials," *Composites, Part B*, Vol. 30, No. 8, pp 777-832.

Atkinson, C., and List, R. D., 1978, "Steady State Crack Propagation Into Media with Spatially Varying Elastic Properties," *International Journal of Engineering Science*, Vol. 16, No. 10, pp. 717-730.

Bao, G., and Wang, L., 1995, "Multiple Cracking in Functionally Graded Ceramic/Metal Coatings," *International Journal of Solids and Structures*, Vol. 32, No. 19, pp. 2853-2871.

Biner, S. B., 1998, "Characteristics of Interface Cracks in Creep Regime," *Materials Science & Engineering A: Structural Materials: Properties, Microstructure and Processing*, Vol. A244, No. 2, pp. 233-249.

Bassani J. L., and McClintock F A., 1981, "Creep Relaxation of Stress around a Crack Tip," *International Journal of Solids and Structures*, Vol. 17, No. 5, pp. 479-492.

Drake, J. T., Williamson, R. L., and Rabin, B. H., 1993, "Finite Element Analysis of Thermal Residual Stresses at Graded Ceramic-Metal Interfaces. Part II. Interface Optimization for Residual Stress Reduction," *Journal of Applied Physics*, Vol. 74, No. 2, p. 1321.

Eischen, J. W., 1987, "Fracture of Nonhomogeneous Materials," *International Journal of Fracture*, Vol. 34, No. l, pp 3-22.

Erdogan, F., 1995, "Fracture Mechanics of Functionally Graded Materials," *Composites Engineering*, Vol. 5, No. 7, pp. 753-770.

Goldberg, R. K., and Hopkins, D. A., 1995, "Application of the Boundary Element Method to the Micromechanical Analysis of Composite

Materials," *Computers and Structures*, Vol. 56, No. 5, pp. 721-731.

Goldman, N. L., and Hutchinson, J. W., 1975, "Fully Plastic Crack Problems the Center-Cracked Strip under Plane Strain," *International Journal of Solids and Structures*, Vol. 11, No. 5, pp. 575-591.

Konda, N., and Erdogan, F., 1994, "Mixed Mode Crack Problem in a Nonhomogeneous Elastic Medium," *Engineering Fracture Mechanics*, Vol. 47, No. 4, pp 533-545.

Moran, B, and Shih, C. F., 1987, "Crack Tip and Associated Domain Integrals from Momentum and Energy Balance," *Engineering Fracture Mechanics*, Vol. 27, No. 6, pp. 615-642.

Niino, M., and Maeca, S., 1990, "Recent Development Status of Functionally Gradient Materials," *ISIJ International*, Vol. 30, No. 9, pp. 699-703.

Noda, N., and Jin, Z-H., 1993, "Thermal Stress Intensity Factors for a Crack in a Strip of a Functionally Gradient Material," *International Journal of Solids and Structures*, Vol. 30, No. 8, pp 1039-1056.

Rice, J. R., and Rosengren, G. F., 1968, "Plane Strain Deformation near a Crack Tip in a Power-Law Hardening Material," *Journal of Mechanics and Physics of Solids*, Vol. 16, No. 1, pp. 1-16.

Sih, G. C., 1974, "Strain-Energy-Density Factor Applied to Mixed Mode Crack Problems," *International Journal of Fracture*, Vol. 10, No. 3, pp. 305-321.

Tu, S. T., 2002, "Creep Behavior of Crack near Bi-Material Interface Characterized by Integral Parameters," *Theoretical and Applied Fracture Mechanics*, Vol. 38, No. 2, pp. 203-209.

Williamson, R. L., Rabin, B. H., and Byerly, G. E., 1995, "FEM Study of the Effects of Interlayers and Creep in Reducing Residual Stresses and Strains in Ceramic-Metal Joints," *Composites Engineering*, Vol. 5, No. 7, pp. 851-863.

Zhang, S. Y., and Leech, C. M., 1985, "Use of Inhomogeneous Finite Elements for the Prediction of Stress in Rope Terminations," *Engineering Computations (Swansea, Wales)*, Vol. 2, No. 1, pp. 56-62.

Manuscript Received: Jun. 18, 2004
and Accepted: Jul. 02, 2004